JCTC Journal of Chemical Theory and Computation

Computational Requirements for Simulating the Structures and Proton Activity of Silicaceous Materials

Yuan Zhang, Zhen Hua Li, and Donald G. Truhlar*

Department of Chemistry and Supercomputing Institute, University of Minnesota, Minneapolis, Minnesota 55455-0431

Received September 18, 2006

Abstract: Structures of disiloxane and silanol and the energetics of their protonation, deprotonation, and proton exchange reactions have been studied with 14 density functionals in combination with eight basis sets. The geometries optimized by these 112 density functional methods are compared to those obtained by the second-order Møller−Plesset perturbation theory and the coupled cluster method, and the performance of all these methods on energetics is evaluated with benchmark Weizmann-1w results. The most accurate density functional for both geometries and energetics is M05-2X. Polarized augmented triple-ζ basis sets are found to be about a factor of 3−4 more accurate than polarized augmented double-ζ basis sets.

1. Introduction

Silicon is abundant in the earth's crust, where it occurs mainly as silica (silicon dioxide) and silicates. There have been many experimental and theoretical investigations of crystalline[1−12] and amorphous[13−22] silicates because of their importance in materials science, geophysics, and technology. In addition, fabricated silaceous mesoporous materials are receiving considerable attention for use and potential use as catalytic nanoreactors and nanotechnological compounds.[23−25] The fundamental structural building blocks of a variety of silica-containing materials are also found in small molecules, which may therefore serve as useful model compounds. In particular, disiloxane ($H_3Si-O-SiH_3$, Figure 1)[26−28] exhibits Si−O bond lengths and Si−O−Si bond angles that are virtually the same as those observed in bulk silica and silicates,[29] and the Si−OH hydroxyl group of silanol (H_3-Si−OH, Figure 2)[30−32] is a molecular mimic of the group found on the surfaces[33] and at the defect sites[34] of hydrous silica and zeolitic materials. These geometric features are very important in zeolites because they control the acidity of the lattice. Silicates and related aluminosilicate materials are major constituents of hydrothermal flows and play an important role in magmatic flow in the earth's crust; they have therefore been investigated extensively by many geologists.[35−37] The incorporation of H in silica is critical for its role in subducting oceanic crust.[38] Proton conduction in water-containing silica, the use of water as a defect passivant in semiconductor devices (and related applications),[39] and the presence of water in optic fibers[40] underline the technological importance of proton energetics in silicates.

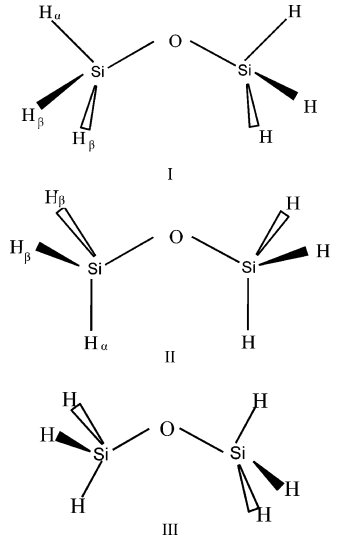

Figure 1. The three conformers of disiloxane.

Molecular force fields have been shown to be useful for reproducing the bulk properties of silica polymorphs, especially when the potential function was derived from extended-basis-set quantum mechanical electronic structure calcula-

* Corresponding author fax: 1-(612) 626-9390; e-mail: truhlar@umn.edu.

10.1021/ct6002884 CCC: $37.00
Published on Web 02/02/2007

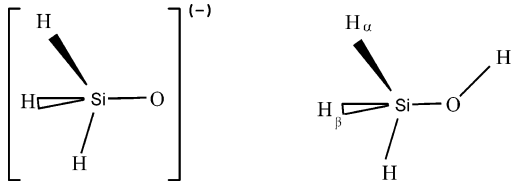

Figure 2. The structures of the silanol anion and silanol.

tions.[41] In fact, it is well-known that modeling silicon-containing compounds requires careful consideration of basis sets.[42] Advances in computational science allow quantum mechanical methods to be applied with large basis sets and high levels of theory to small systems and moderate basis sets and moderate levels of theory to larger and larger cluster models.[43−48] A validation study designed to show the computational requirements for modeling silicaceous material is a key starting point for examining the required levels of theory and sizes of basis sets. In particular, density functional theory (DFT) can be used to test the large number of molecular mechanics force fields[13,32,41,49−56] that have been proposed for silica, silicates, alkylsilanes, and disiloxane polymers. This is especially important because disiloxane has proven to be a highly useful benchmark for the accuracy of electronic structure methods for use in zeolite calculations.[27,57,58] Disiloxane serves not only as a model for silicone oxides and silicates but also as a model for polymeric organosiloxanes such as silicone oil[13,55,59,60] (polydimethylsiloxane polymers). In the present work, we use disiloxane and silanol as prototype molecules for testing and validating quantum mechanical computational methods.

We also study protonation and deprotonation of these two model systems, silanol and dimethylsiloxane. Knowledge of proton affinities is essential for studying proton transport in minerals, and the protonation of dimethylsiloxane may be considered to be a model for the protonation of an acid site in an all-silica zeolite or for diffusion of hydrogen in acidic silica or zeolites.[61−63]

For direct dynamics simulations, one wants to use the smallest possible basis set that yields the required accuracy, so it is essential to test both small and larger basis sets systematically. Many of the older studies of basis set extension were based on[42,64] wave function theory (WFT), but it is now widely recognized that DFT provides a more efficient and more accurate electronic structure approach for direct dynamics calculations. For example, both the B3LYP and M05-2X density functionals are more accurate than second-order-perturbation WFT.[65] Furthermore, it is now known that DFT has different[66−70] and sometimes smaller basis set requirements than WFT. It is also known that density functionals that are optimum for main-group chemistry may be very inaccurate for metals and vice versa,[71] with less systematic tests available for semiconductor elements like Si. These considerations motivate a systematic exploration of the accuracy of various density functionals and basis sets for prototype Si-containing molecules.

Both experimental and theoretical studies have shown that it is very difficult to determine with reasonable confidence the structures of disiloxane and silanol, in particular, the important Si−O−Si bond angle and the Si−O bond distance.

Table 1. Summary of the DFT Methods Assessed in This Study

	X[a]	year	type	ref(s)
HCTH	0	1998	local[b]	78−80
M06-L	0	2006	local	82
mPWPW	0	1998	local	83, 84
PBE	0	1996	local	85
VSXC	0	1998	local	89
MPWLYP1M	5	2005	HDFT[c]	70
TPSSh	10	2003	HDFT	87, 88
B3LYP	20	1994	HDFT	74, 75, 77
B97−1	21	1998	HDFT	78
B1LYP	25	1997	HDFT	74−76
M05	28	2005	HDFT	81
MPW1B95	31	2004	HDFT	53, 56, 78
PW6B95	46	2005	HDFT	86
M05-2X	56	2006	HDFT	71

[a] *X* denotes the percentage of Hartree−Fock exchange in the functional. [b] The term local denotes local density functional theory. [c] HDFT denotes hybrid density functional theory.

The geometries of these molecules obtained by theoretical methods are highly sensitive to the sophistication of the calculations. DFT is a powerful means by which zeolite structure, acidity, and reactivity can be elucidated.[72,73] DFT methods can provide very accurate results for geometries, energies, and other properties. However, the computational requirements of DFT are less demanding than those for wave function theory methods of comparable accuracy, allowing one to efficiently study the large systems needed for the realistic modeling of zeolitic materials. The accuracy of the DFT calculations depends on a variety of factors; the most important of these are the flexibility of the basis set and the form of the exchange-correlation functional. A larger, more flexible basis set gives a better description of the electron density but is computationally more demanding.

In the present study, the accuracy of 14 density functionals and eight basis sets was evaluated by calculating the geometries of disiloxane and silanol and the energies of their protonation/deprotonation and proton-transfer reactions. The 14 DFT functionals that we assess are B1LYP,[74−76] B3LYP,[74,75,77] B97-1,[78] HCTH,[78−80] M05,[81] M05-2X,[71] M06-L,[82] MPW1B95,[53,56,78] MPWLYP1M,[70] mPWPW,[83,84] PBE,[85] PW6B95,[86] TPSSh,[87,88] and VSXC.[89] All DFT methods in the present paper are listed in Table 1, ordered by the percentage *X* of Hartree−Fock (HF) exchange in the functional and, for a given *X*, are in alphabetical order.

The eight basis sets evaluated here include five polarized double-ζ basis sets, 6-31+B**,[90] 6-31+G**,[91] MIDI!,[92−94] MIDIX+,[95]and aug-pc1,[67,69] and three polarized triple-ζ basis sets, aug-cc-pV(T+d)Z,[96] aug-pc2,[67,69] and MG3S.[68] The aug-pc1 and aug-pc2 basis sets were created[67,69] expressly for use with DFT, so it is particularly interesting to test their accuracy and efficiency. Note that MIDI! is called MIDIX in the *Gaussian* program.

Two ab initio WFT methods, namely, Møller−Plesset second-order perturbation theory (MP2)[97] and coupled cluster theory with single and double excitations (CCSD),[98] were also used to optimize the geometries. The CCSD geometries are used as a benchmark in some cases (see below), but the

Table 2. Number of Contracted and Primitive Basis Functions Used in the Calculation Of Protonated Disiloxane ($H_6Si_2OH^+$)[a]

	MIDI!	MIDIX+	6-31+B**	6-31+G**	aug-pc1	av (PDZ)	MG3S	aug-pc2	aug-cc-pV(T+d)Z	av (PTZ)
contracted	64	76	97	100	140	95.4	205	307	317	276.3
primitive	108	120	193	193	274	177.6	293	508	536	445.7
ref(s)	92−94	95	90	91	66, 68		67	66, 68	96	

[a] PDZ denotes polarized double-ζ; PTZ denotes polarized triple-ζ; av denotes average.

MP2 calculations were carried out only for comparison purposes. High-level benchmark calculations were performed using the multicoefficient correlation method MCCM/3,[99] the balanced multicoefficient method BMC−CCSD,[90] and the very accurate multilevel Weizmann-1w (W1w)[100−102] method with fixed geometries calculated at the CCSD/MG3S and B97-1/aug-cc-pV(T+d)Z levels. B97-1 is the recommended method for geometry optimization of large molecules in the W2 protocol; see ref 101 for more information. Furthermore, aug-cc-pV(T+d)Z[96] is recommended by Martin[102] for geometry optimization in the W1w and W2w theories. To check that these geometries are sufficiently reliable for the W1w calculations, we also carried out W1w calculations at CCSD/MG3S geometries.

Parthiban and Martin[103] studied the accuracy of W1 and W2 theory for proton affinities and found that W1 "can basically be considered converged for this purpose"; in fact, they concluded that the uncertainty in W1 proton affinities is "considerably lower than that of the experimental values". Similar conclusions apply to W1w. Thus, our tests of the accuracy for proton affinities should be quite reliable.

2. Computational Details

All DFT, MP2, and CCSD energies and geometry optimizations were carried out using the *Gaussian 03*[104] and *MN-GFM*[105] programs, and the W1w calculations (using the Douglas−Kroll[106] relativistic correction as in ref 102) were carried out using the *MOLPRO*[107] program. H_6Si_2O (see Figure 1), H_3SiOH (see Figure 2), and the corresponding protonated and deprotonated molecules were fully optimized using the 14 DFT methods in combination with a series of basis sets. Vibrational frequency calculations were performed for all the stationary points, using each method and basis set, and these calculations verified that all structures are minima (no imaginary frequencies). We allowed the molecules complete flexibility during the analytical gradient geometry optimization except for reasonable symmetry constraints, for example, C_{2v} and C_s for disiloxane, C_s for silanol, and C_{3v} for the deprotonated silanol anion (H_3SiO^-). Because of the expected very shallow potential energy profile for fluctuations of the Si−O−Si bond angle of disiloxane, the geometry optimization criteria were set to stringent values (keyword ''opt=tight" in *Gaussian 03*). The integration grid used is a pruned (99, 590) grid ("ultrafine" as defined in *Gaussian 03*).

To illustrate the relative sizes of the various basis sets, Table 2 lists the total number of basis functions used in the calculation of protonated disiloxane.

3. Results and Discussion

Before considering our results, it is useful to note which levels of theory and basis sets have been used by other workers for some of the more accurate available studies of Si-containing compounds. Nachtigall et al.[108] employed the 6-311+G(3df,2pd) level and basis sets and found that the B3LYP functional is more accurate than local functionals for Si−Si bond cleavage and H_2 elimination from silanes (1996). Eichler et al.[109] used HF theory with a triple-ζ polarized basis set on O and a double-ζ polarized basis set on H and Si for an active site surrounded by a molecular mechanics environment (1997). Chatterjee et al.[34] used B3LYP/DNP for cluster calculations, where DNP is similar in quality to 6-31G(d,p) (1998). Demuth et al.[61] used the local PW91 density functional with a projector-augmented plane wave basis for periodic boundary condition calculations on mordenite (2000). Tossell and Sahaia[110] calculated $Si(OH)_3O^-\cdot 4H_2O$ at the MP2/6-311+G(2d,p)//HF/6-311+G-(2d,p) level. Walsh et al.[111] carried out cluster calculation where the active site was treated by B3LYP/6-31G(d) and the rest of the cluster by HF/STO-3G (2000). Tielens et al.[28] used density functional theory with aug-cc-pV*X*Z (*X* = D, T, Q) basis sets for calculation on silanol and disiloxane (2001). They found that B3LYP and B3PW91 performed the best, out of six functionals studied, and that they gave very similar results. Yuan et al.[112] carried out ZSM-5 zeolite calculations by ab initio HF or DFT methods (2002). Bussai et al.[113] carried out calculations on clusters at the HF/6-31G-(d) level (2002). Zwijnenburg et al.[62] carried out calculations on clusters at the B3LYP/6-31G(d) level (2002). Simperler et al.[48] carried out cluster calculations at the PW91/DNP level (2004). Tuma and Sauer[114] carried out cluster calculations with a PBE density functional and a plane wave basis set; they also used a combined MP2/DFT method (2004). Saengsawang et al.[33] carried out cluster calculations at the B3LYP/6-31++G(d,p) level (2005). Tossell[115] calculated the dimerization of silanol with B3LYP and MP2 using the 6-311+G(2d,p) basis set and with higher-level WFT calculations with smaller basis sets and low-level geometrics (2005). Ginhoven et al.[116] calculated water reactions in silica with the PW91 density functional and a plane wave basis set. Bakk et al.[117] modeled extended systems containing siloxane building blocks at the B3LYP/6-311+G(3df,3dp)//B3LYP/6-31+G(d) and MP2/6-311+G(3df,3pd)//MP2/6-31+G(d) levels (2006). Since most of the studies of silicaceous compounds used polarized double-ζ basis sets, it will be interesting to see if this is accurate enough.

3.1. Geometries of Disiloxane and Silanol. Disiloxane provides the simplest molecular representation of the key internal coordinates of the zeolite framework. This molecule has three possible conformers, two with C_{2v} symmetry, namely, the doubly staggered (I) and the doubly eclipsed (II), and the third with C_s symmetry (III), as shown in Figure 1. In the doubly staggered conformation, one of the

Table 3. Benchmark Values of Key Geometric Parameters and Dipole Moments for Silanol and Disiloxane (Distances in Å, Angles in Degrees, Dipole Moments in Debyes)

	silanol	disiloxane
	CCSD/MG3S	experiment
Si−O	1.645	1.634[29]
Si−O−H	118.6	
Si−O−Si		151.2[120]
μ	1.327	0.24[129]

hydrogens of both silyl groups is in a staggered position with respect to the opposite Si−O bond. In the doubly eclipsed conformation, both silyl groups are rotated by 180° relative to the doubly staggered position. Conformer III can be obtained by rotating one of the silyl groups in either conformer I or II by 180°. Earlier studies on conformers I and II indicate that conformer I is lower in energy.[29] This agrees with the experimental results on disiloxane crystals, which imply that disiloxane exhibits a distorted C_{2v} structure similar to that of conformer I.[30,118]

For disiloxane, both experimental and theoretical studies indicate that the energy change with respect to the Si−O−Si angle is very small, and the energy difference from the bent structure to the linear structure is only about 0.3 kcal/mol.[119,120] This extremely flat energy surface has resulted in large uncertainties in the experimental values of the Si−O−Si angle. An electron diffraction[29] study of gaseous disiloxane reported an angle of 144.1°; an X-ray crystal structure (solid phase)[121] of hexamethyl disiloxane gives 142.1°; a Raman/IR study[119] on crystalline disiloxane gave an angle of 149 ± 2°, and a more recent low-frequency Raman study[120] suggested a Si−O−Si angle of 151.2°. The key geometric parameters and dipole moments for silanol and disiloxane, both benchmark values and those predicted by the various levels of theory, are given in Tables 3−5.

In the present study, the results of most methods yield conformer I as stable, in agreement with early studies; however, for some methods, in particular, M05-2X/MG3S, M05-2X/aug-pc2, M05-2X/aug-cc-pV(T+d)Z, M06-L/MG3S, M06-L/aug-pc2, M06-L/aug-cc-pV(T+d)Z, and the VSXC functional with all basis sets except MIDIX+, conformer I is not stable; in all of these cases, conformer II is stable and was used for the calculation in the tables. At most levels, conformer III is a first-order transition state. We must emphasize that the potential energy surface of disiloxane is very flat with respect to the rotation of the silyl groups, and the absolute energy differences between the three conformers are very small, usually just a few hundredths of a kilocalorie per mole. As a result, the experimental results may correspond to an almost equal mixture of the different conformers.

In contrast to the considerable amount of data on disiloxane, there are no experimental data available on silanol, probably because it has a strong tendency to condense into disiloxane.[27] The benchmark values in Table 3 are from theory for silanol and from experimental results for disiloxane. The theoretical results for silanol are carried out with an augmented polarized triple-ζ basis set, in particular, by CCSD/MG3S. The use of geometries calculated at this level is motivated by previous experience in achieving a compromise of affordability and reliability for the geometry optimization of molecules with six or more atoms. It may also be justified by systematic work on smaller molecules. Consider, for example, the recent systematic studies of geometries for compounds containing second-row atoms by Coriani et al.[123] The found that bond lengths at the CCSD/cc-pVTZ level were not systematically improved by increasing the level to CCSD(T) or by increasing the basis to cc-pVQZ, and bond angles were not systematically improved by increasing the basis to cc-pVTZ. They found that the mean unsigned errors in their calculated CCSD/cc-pVTZ bond lengths and bond angles are 0.008 Å and 0.4°, respectively. Their average error for CCSD bond lengths would probably have been smaller if they had a third tighter *d* function for second-row atoms such as those in the MG3S basis, which does not suffer from this known deficiency of the cc-pVTZ and aug-cc-pVTZ basis sets. We note that their study did not include any molecules with more than five atoms (it involved one symmetric penta-atomic molecule, six tetra-atomics, 23 triatomics, and nine diatomics). Thus, conclusions about large molecules are subject to more uncertainty.

In Table 4, we present the values calculated for the equilibrium Si−O−Si and Si−O−H angles of disiloxane and silanol at various levels of theory. Results in the table indicate that the Si−O−Si angle is extremely sensitive to both the method and the basis set. In extreme cases, Si−O−Si is even predicted to be linear. For the polarized double-ζ 6-31+G**, MIDIX+, and 6-31+B** basis sets, 11, 7, and 2 out of 14 functionals, respectively, give a linear structure, while none of them give linear structures for the MIDI! and aug-pc1 basis sets. Grigoras and Lane have shown that the Si−O−Si angle is very sensitive to the values of the *d*-orbital exponent on Si,[122] which may explain the poor performance of some polarized double-ζ basis sets. MIDI! and aug-pc1 are the two best polarized double-ζ basis sets for the bond angle in disiloxane. Polarized triple-ζ basis sets generally give larger Si−O−Si angles than polarized double-ζ basis sets except for those polarized double-ζ basis sets giving linear structures. However, none of these polarized triple-ζ basis sets give a linear structure. Among the three polarized triple-ζ basis sets, except at the VSXC level, MG3S always gives the largest Si−O−Si angle, while aug-pc2 gives the smallest angle. It has been suggested by Nicholas et al. that, since the experimental values are not measured at 0 K, a thermal correction of about −5° should be applied to the experimental value.[30] After the correction, all of the theoretical values obtained using the polarized triple-ζ basis sets are further away from the experimental value. Since both of the available high-level ab initio methods, in particular, the present CCSD/MG3S calculation and the previous[124] CPF calculation, give a value greater than 152°, the uncorrected 151.2° of the latest measurement is perhaps the most accurate value. Examining the results given by the polarized triple-ζ basis sets indicates that all pure functionals give smaller Si−O−Si angles than the hybrid functionals. If one accepts that the recent experimental value of 151.2° is the most accurate

Table 4. Si−O−H and Si−O−Si Bond Angles of Silanol and Disiloxane (in Degrees)

	HCTH								M06-L							
	MIDI!	MIDIX+	6-31+B**	6-31+G**	aug-pc1	MG3S	aug-pc2	aug-cc-pV(T+d)Z	MIDI!	MIDIX+	6-31+B**	6-31+G**	aug-pc1	MG3S	aug-pc2	aug-cc-pV(T+d)Z
Si−O−H	112.3	115.7	117.3	117.4	116.0	117.8	117.9	117.7	113.7	115.9	118.0	117.7	116.0	118.5	117.7	118.1
Si−O−Si	142.1	143.7	140.7	146.6	138.4	149.5	148.1	148.7	134.2	136.6	143.6	180.0	139.1	153.8	148.6	153.5
MUE[a]	7.7	5.2	6.0	2.9	7.7	1.3	1.9	1.7	11.0	8.6	4.1	14.8	7.4	1.4	1.8	1.4
	mPWPW								PBE							
	MIDI!	MIDIX+	6-31+B**	6-31+G**	aug-pc1	MG3S	aug-pc2	aug-cc-pV(T+d)Z	MIDI!	MIDIX+	6-31+B**	6-31+G**	aug-pc1	MG3S	aug-pc2	aug-cc-pV(T+d)Z
Si−O−H	112.2	115.6	117.3	117.2	115.8	117.5	117.2	117.1	111.8	115.2	117.0	116.9	115.6	117.2	117.0	116.9
Si−O−Si	139.0	140.8	142.4	180.0	137.4	148.6	145.4	146.4	137.0	138.1	139.2	145.0	135.6	145.9	143.6	144.3
MUE[a]	9.3	6.7	5.1	15.1	8.3	1.9	3.6	3.1	10.5	8.3	6.8	4.0	9.3	3.4	4.6	4.3
	VSXC								MPWLYP1M							
	MIDI!	MIDIX+	6-31+B**	6-31+G**	aug-pc1	MG3S	aug-pc2	aug-cc-pV(T+d)Z	MIDI!	MIDIX+	6-31+B**	6-31+G**	aug-pc1	MG3S	aug-pc2	aug-cc-pV(T+d)Z
Si−O−H	114.1	117.7	120.1	120.1	118.1	119.7	119.7	119.4	112.9	116.5	118.2	118.2	117.1	118.7	118.5	118.4
Si−O−Si	134.3	180.0	134.1	135.0	131.8	135.8	136.3	136.2	144.4	146.4	147.3	180.0	141.8	153.8	150.3	151.6
MUE[a]	10.7	14.7	9.3	8.9	10.0	8.2	8.0	7.9	6.3	3.5	2.1	14.6	5.5	1.4	0.5	0.3
	TPSSh								B3LYP[b]							
	MIDI!	MIDIX+	6-31+B**	6-31+G**	aug-pc1	MG3S	aug-pc2	aug-cc-pV(T+d)Z	MIDI!	MIDIX+	6-31+B**	6-31+G**	aug-pc1	MG3S	aug-pc2	aug-cc-pV(T+d)Z
Si−O−H	113.5	116.9	118.6	118.4	116.6	118.5	118.3	118.1	113.6	117.1	119.0	119.0	117.7	119.5	119.2	119.1
Si−O−Si	145.0	180.0	149.9	180.0	140.6	155.6	151.0	152.0	145.3	180.0	180.0	180.0	143.8	158.9	152.2	156.6
MUE[a]	5.7	15.3	0.7	14.5	6.3	2.3	0.3	0.7	5.5	15.2	14.6	14.6	4.2	4.3	0.8	2.9
	B97-1								B1LYP							
	MIDI!	MIDIX+	6-31+B**	6-31+G**	aug-pc1	MG3S	aug-pc2	aug-cc-pV(T+d)Z	MIDI!	MIDIX+	6-31+B**	6-31+G**	aug-pc1	MG3S	aug-pc2	aug-cc-pV(T+d)Z
Si−O−H	112.8	116.3	118.3	118.3	116.7	118.5	118.3	118.0	113.7	117.3	119.2	119.2	117.8	119.7	119.4	119.3
Si−O−Si	139.5	143.2	143.5	180.0	138.8	151.3	148.6	149.9	146.2	180.0	180.0	180.0	144.5	160.5	155.7	158.1
MUE[a]	8.7	5.2	4.1	14.6	7.2	0.1	1.5	0.9	5.0	15.1	14.7	14.7	3.8	5.2	2.6	3.8
	M05								MPW1B95							
	MIDI!	MIDIX+	6-31+B**	6-31+G**	aug-pc1	MG3S	aug-pc2	aug-cc-pV(T+d)Z	MIDI!	MIDIX+	6-31+B**	6-31+G**	aug-pc1	MG3S	aug-pc2	aug-cc-pV(T+d)Z
Si−O−H	113.7	117.1	119.2	119.3	117.5	120.0	119.2	119.1	113.6	117.1	119.2	119.2	117.4	119.3	119.1	118.9
Si−O−Si	141.6	142.4	144.1	180.0	139.0	158.4	153.0	156.7	143.0	180.0	152.0	180.0	141.4	157.5	153.0	155.6
MUE[a]	7.3	5.2	3.9	14.7	6.7	4.3	1.2	3.0	6.7	15.2	0.7	14.7	5.5	3.5	1.1	2.3
	PW6B95								M05-2X							
	MIDI!	MIDIX+	6-31+B**	6-31+G**	aug-pc1	MG3S	aug-pc2	aug-cc-pV(T+d)Z	MIDI!	MIDIX+	6-31+B**	6-31+G**	aug-pc1	MG3S	aug-pc2	aug-cc-pV(T+d)Z
Si−O−H	113.5	117.1	119.2	119.2	117.4	119.3	119.1	119.0	113.8	117.8	106.1	120.4	118.3	120.4	120.1	120.2
Si−O−Si	143.8	180.0	152.3	180.0	142.0	157.7	153.2	155.7	142.3	180.0	146.5	180.0	140.1	156.7	152.2	156.2
MUE[a]	6.3	15.2	0.8	14.7	5.2	3.6	1.2	2.4	6.9	14.8	8.6	15.2	5.7	3.6	1.2	3.3

	MP2							
	MIDI!	MIDIX+	6-31+B**	6-31+G**	aug-pc1	MG3S	aug-pc2	aug-cc-pV(T+d)Z
Si−O−H	113.0	117.0	118.8	118.7	116.4	118.3	118.2	117.8
Si−O−Si	139.9	144.1	144.9	180.0	137.3	151.2	147.7	148.7
MUE[a]	8.5	4.4	3.2	14.4	8.0	0.2	2.0	1.7

[a] MUE denotes mean unsigned error. [b] For comparison, we note the following results of Tielens et al.:[28] 116.4, 135.6, and 8.9 with aug-cc-pVDZ; 118.5, 150.2, and 0.6 with aug-cc-pVTZ; and 119.1, 152.4, and 0.9 with aug-cc-pVQZ.

(and this value was selected as the benchmark in Table 3), then hybrid functionals perform better.

The Si−O−H angle was found to be the most sensitive geometrical parameter of silanol. MIDI! always gives the smallest angle, deviating from the high-level CCSD result of Table 3 by almost 5°, while other polarized double-ζ basis sets perform fairly well. Except for the M05 functional, the largest difference among the angles given by the three polarized triple-ζ basis sets never exceeds 0.4°.

The MUEs in Table 4 are the mean unsigned errors in these two bond angles. Not unexpectedly, most of the MUEs of the polarized triple-ζ basis sets are smaller than those of the polarized double-ζ basis sets. The performance of the three polarized triple-ζ basis sets depends on the functional.

Table 5. Mean Unsigned Error (in Å) of the Si−O Bond Distances in Silanol and Disiloxane

	PDZ[a]					PTZ[a]		
	MIDI!	MIDIX+	6-31+B**	6-31+G**	aug-pc1	MG3S	aug-pc2	aug-ccpV(T+d)Z
HCTH	0.028	0.044	0.040	0.032	0.040	0.007	0.012	0.011
M06-L	0.017	0.028	0.025	0.011	0.027	0.007	0.003	0.005
mPWPW	0.032	0.040	0.040	0.020	0.040	0.010	0.010	0.010
PBE	0.033	0.049	0.046	0.039	0.047	0.016	0.021	0.020
VSXC	0.020	0.027	0.032	0.026	0.033	0.007	0.010	0.009
MPWLYP1M	0.028	0.046	0.043	0.031	0.044	0.014	0.018	0.017
TPSSh	0.021	0.030	0.032	0.020	0.034	0.004	0.007	0.006
B3LYP[b]	0.019	0.029	0.025	0.019	0.032	0.005	0.010	0.004
B97−1	0.023	0.037	0.034	0.020	0.034	0.003	0.007	0.007
B1LYP	0.017	0.028	0.024	0.018	0.030	0.005	0.004	0.004
M05	0.019	0.036	0.029	0.016	0.030	0.006	0.004	0.004
MPW1B95	0.010	0.019	0.020	0.009	0.022	0.009	0.004	0.006
PW6B95	0.012	0.020	0.021	0.009	0.023	0.008	0.003	0.003
M05-2X	0.014	0.025	0.027	0.016	0.029	0.002	0.003	0.002
MP2	0.022	0.041	0.041	0.024	0.044	0.003	0.009	0.009

[a] PDZ denotes polarized double-ζ; PTZ denotes polarized triple-ζ. [b] For comparison, Tielens et al.[28] obtained 0.056 with aug-cc-pVDZ, 0.015 with aug-cc-pVTZ, and 0.007 with aug-cc-pVQZ.

For some functionals, one basis set gives smaller MUEs than others, while for some other functionals, another basis set gives smaller MUEs. In most cases, the MUEs of 6-31+B** are the smallest among the polarized double-ζ basis sets. Among all the possible combinations of functionals and basis sets, TPSSh/aug-pc2 and MPWLYP1M/aug-cc-pV(T+d)Z most closely reproduce the CCSD/MG3S and experimental results (MUE = 0.29 and 0.33°, respectively).

In Table S1 of the Supporting Information, we present the calculated equilibrium Si−O bond lengths of disiloxane and silanol at various levels of theory, and in Table 5, we present the mean unsigned error (compared to the experimental value for disiloxane and the theoretical CCSD/MG3S value for silanol), averaged over these two bond lengths. For the Si−O bond lengths of disiloxane, polarized triple-ζ basis sets always give shorter bond distances than polarized double-ζ for a given functional, closer to the experimental value of 1.634 Å and the high-level CCSD/MG3S result of 1.626 Å. For the Si−O bond lengths of silanol, among the five polarized double-ζ basis sets, MIDI! always gives the shortest bond distances, closer to the values given by the polarized triple-ζ basis sets. All density functionals perform very well with small MUEs. Among the five polarized double-ζ basis sets, MIDI! performs the best. The MUEs of the polarized triple-ζ basis sets are all smaller than those of the polarized double-ζ basis sets. The MG3S basis set performs better than the other two polarized triple-ζ basis sets. Taking only polarized triple-ζ basis sets into consideration, the M05-2X and B1LYP functionals have the best overall performances for the Si−O distances of dixiloxane and silanol.

3.2. Dipole Moments of Disiloxane and Silanol. Zwijnenburg et al.[62] studied the polarity of Si−O bonds in siliceous materials by calculating partial atomic changes. They found that two different methods of extracting such changes from DFT orbitals gave quite different results. We prefer, therefore, at least in the present study, to avoid such artificial quantities. We will instead use the dipole moment, an unambiguous physical observable, to gauge the accuracy of our charge distributions. The dipole moment depends strongly on the geometry, the basis set, and the density functional. The Si−O−Si bond angle plays an especially important role in determining the value of the dipole moment, which reaches a minimum (zero) for disiloxane when the Si−O−Si angle is linear.

In Table 6, we present the calculated dipole moments of disiloxane and silanol at various levels of theory. Examining the MUEs, MIDI! and aug-pc1 have the smallest MUEs among the five polarized double-ζ basis sets with all functionals. For the polarized triple-ζ basis sets, the MUEs of the MG3S basis set are always the smallest. Taking only polarized triple-ζ basis sets into consideration, the M05-2X functional has the best performance for dipole moments. Among all the combinations of functionals and basis sets, TPSSh/MG3S and M05-2X/MG3S are the best methods, with MUEs of just 0.014 and 0.008 D, respectively. Other hybrid functionals also perform very well.

3.3. Protonation/Deprotonation and Proton-Transfer Reactions. In this section, we discuss proton-transfer reactions. A proton-transfer reaction involves protonating the proton acceptor and deprotonating the proton donor. The proton affinities of both disiloxane and silanol are sensitive to the theoretical treatment. However, the accuracy with which we can calculate protonation energy is important for work with zeolites. The three possible proton-transfer reactions involving disiloxane and silanol are listed in Figure 3. The three reactions contain two protonation processes, $H^+ + (H_3Si)_2O \rightarrow (H_3Si)_2OH^+$ and $H_3SiOH + H^+ \rightarrow H_3SiOH_2^+$, and one deprotonation process, $H_3SiOH \rightarrow H^+ + H_3SiO^-$.

In Table 7, the W1w proton affinities of H_3SiO^-, H_3SiOH, and $(H_3Si)_2O$ are listed along with results from other accurate theoretical calculations and experiments where available. The G1 and G2 results are expected to be accurate to 2−3 kcal/mol, which is reasonably accurate but not as accurate as W1w. The W1w proton affinity of H_3SiO^- is 363.7 kcal/mol. The best available ab initio calculated value is 364.1 ± 1.1 kcal/mol.[125] With zero-point energy included, the proton affinity of the silanol anion is 355.7 kcal/mol. The

Table 6. Dipole Moments of Silanol and Disiloxane (in Debye)

	HCTH								M06-L							
	MIDI!	MIDIX+	6-31+B**	6-31+G**	aug-pc1	MG3S	aug-pc2	aug-cc-pV(T+d)Z	MIDI!	MIDIX+	6-31+B**	6-31+G**	aug-pc1	MG3S	aug-pc2	aug-cc-pV(T+d)Z
silanol	1.478	1.538	1.467	1.472	1.242	1.277	1.250	1.249	1.653	1.548	1.498	1.493	1.275	1.315	1.272	1.274
disiloxane	0.330	0.532	0.556	0.461	0.427	0.251	0.256	0.237	0.203	0.396	0.479	0.000	0.436	0.219	0.234	0.219
MUE[a]	0.120	0.252	0.228	0.183	0.136	0.030	0.047	0.041	0.181	0.188	0.205	0.203	0.124	0.017	0.031	0.037
	mPWPW								PBE							
	MIDI!	MIDIX+	6-31+B**	6-31+G**	aug-pc1	MG3S	aug-pc2	aug-cc-pV(T+d)Z	MIDI!	MIDIX+	6-31+B**	6-31+G**	aug-pc1	MG3S	aug-pc2	aug-cc-pV(T+d)Z
silanol	1.515	1.541	1.498	1.495	1.257	1.292	1.256	1.257	1.515	1.543	1.495	1.495	1.255	1.290	1.256	1.257
disiloxane	0.327	0.564	0.566	0.000	0.471	0.292	0.297	0.288	0.336	0.601	0.604	0.515	0.477	0.306	0.309	0.300
MUE[a]	0.137	0.269	0.248	0.204	0.151	0.043	0.064	0.059	0.142	0.289	0.266	0.221	0.155	0.052	0.070	0.065
	VSXC								MPWLYP1M							
	MIDI!	MIDIX+	6-31+B**	6-31+G**	aug-pc1	MG3S	aug-pc2	aug-cc-pV(T+d)Z	MIDI!	MIDIX+	6-31+B**	6-31+G**	aug-pc1	MG3S	aug-pc2	aug-cc-pV(T+d)Z
silanol	1.544	1.545	1.468	1.474	1.255	1.299	1.269	1.272	1.500	1.555	1.502	1.503	1.270	1.301	1.263	1.264
disiloxane	0.294	0.005	0.590	0.565	0.445	0.326	0.303	0.294	0.296	0.504	0.492	0.000	0.434	0.250	0.265	0.251
MUE[a]	0.136	0.226	0.245	0.236	0.138	0.057	0.061	0.055	0.114	0.246	0.213	0.208	0.126	0.018	0.044	0.037
	TPSSh								B3LYP[b]							
	MIDI!	MIDIX+	6-31+B**	6-31+G**	aug-pc1	MG3S	aug-pc2	aug-cc-pV(T+d)Z	MIDI!	MIDIX+	6-31+B**	6-31+G**	aug-pc1	MG3S	aug-pc2	aug-cc-pV(T+d)Z
silanol	1.524	1.552	1.504	1.501	1.274	1.308	1.275	1.277	1.509	1.557	1.504	1.505	1.284	1.313	1.280	1.281
disiloxane	0.292	0.000	0.456	0.000	0.440	0.231	0.254	0.244	0.292	0.001	0.000	0.000	0.412	0.200	0.251	0.209
MUE[a]	0.125	0.232	0.197	0.207	0.127	0.014	0.033	0.027	0.116	0.234	0.208	0.209	0.107	0.027	0.029	0.039
	B97-1								B1LYP							
	MIDI!	MIDIX+	6-31+B**	6-31+G**	aug-pc1	MG3S	aug-pc2	aug-cc-pV(T+d)Z	MIDI!	MIDIX+	6-31+B**	6-31+G**	aug-pc1	MG3S	aug-pc2	aug-cc-pV(T+d)Z
silanol	1.507	1.549	1.501	1.502	1.278	1.308	1.277	1.277	1.503	1.559	1.504	1.506	1.288	1.316	1.282	1.284
disiloxane	0.321	0.527	0.538	0.000	0.450	0.258	0.268	0.254	0.286	0.000	0.000	0.000	0.405	0.185	0.218	0.196
MUE[a]	0.130	0.254	0.236	0.207	0.130	0.019	0.039	0.032	0.111	0.236	0.209	0.209	0.102	0.033	0.033	0.044
	M05								MPW1B95							
	MIDI!	MIDIX+	6-31+B**	6-31+G**	aug-pc1	MG3S	aug-pc2	aug-cc-pV(T+d)Z	MIDI!	MIDIX+	6-31+B**	6-31+G**	aug-pc1	MG3S	aug-pc2	aug-cc-pV(T+d)Z
silanol	1.513	1.554	1.515	1.513	1.299	1.322	1.271	1.273	1.510	1.554	1.499	1.500	1.284	1.315	1.284	1.286
disiloxane	0.310	0.529	0.561	0.000	0.464	0.205	0.228	0.192	0.317	0.000	0.556	0.000	0.426	0.206	0.233	0.210
MUE[a]	0.128	0.258	0.254	0.213	0.126	0.020	0.034	0.051	0.130	0.234	0.244	0.206	0.115	0.023	0.025	0.036
	PW6B95								M05-2X							
	MIDI!	MIDIX+	6-31+B**	6-31+G**	aug-pc1	MG3S	aug-pc2	aug-cc-pV(T+d)Z	MIDI!	MIDIX+	6-31+B**	6-31+G**	aug-pc1	MG3S	aug-pc2	aug-cc-pV(T+d)Z
silanol	1.501	1.553	1.495	1.497	1.281	1.310	1.279	1.280	1.483	1.589	1.505	1.511	1.299	1.328	1.298	1.307
disiloxane	0.313	0.000	0.409	0.000	0.423	0.207	0.234	0.211	0.349	0.000	0.483	0.000	0.442	0.237	0.270	0.240
MUE[a]	0.129	0.233	0.178	0.213	0.106	0.019	0.031	0.042	0.146	0.234	0.207	0.206	0.123	0.008	0.037	0.021

	MP2							
	MIDI!	MIDIX+	6-31+B**	6-31+G**	aug-pc1	MG3S	aug-pc2	aug-cc-pV(T+d)Z
silanol	1.581	1.670	1.645	1.638	1.450	1.431	1.403	1.408
disiloxane	0.411	0.590	0.625	0.000	0.614	0.329	0.358	0.357
MUE[a]	0.213	0.347	0.351	0.275	0.248	0.096	0.097	0.099

[a] MUE denotes mean unsigned error. [b] For comparison, Tielens et al.[28] obtained 1.304, 0.554, and 0.169 with aug-cc-pVDZ; 1.278, 0.289, and 0.049 with aug-cc-pVTZ; and 1.276, 0.251, and 0.031 with aug-cc-pVQZ.

G2 result is 356.2 kcal/mol,[126] and the ab initio result is 356.2 ± 2 kcal/mol at 0 K,[125] in agreement with the W1w result. The ΔH°_{298} value calculated using W1w is 355.3 kcal/mol; this calculated value is in good agreement with the experimental value of 352 ± 4 kcal/mol.[127] The W1w proton affinity of silanol is 176.8 kcal/mol. The G2 value is 0.7 kcal/mol higher (177.5 kcal/mol); there is no experimental value for this quantity. The W1w proton affinity of disiloxane is 179.0 kcal/mol, which is the same as the G2 value; again, there is no experimental value for this quantity. Only low-level theoretical calculations have been reported,[126] and these give higher values for the proton affinity. The results in Table 7 indicate that the proton affinities of silanol and disiloxane are nearly the same.

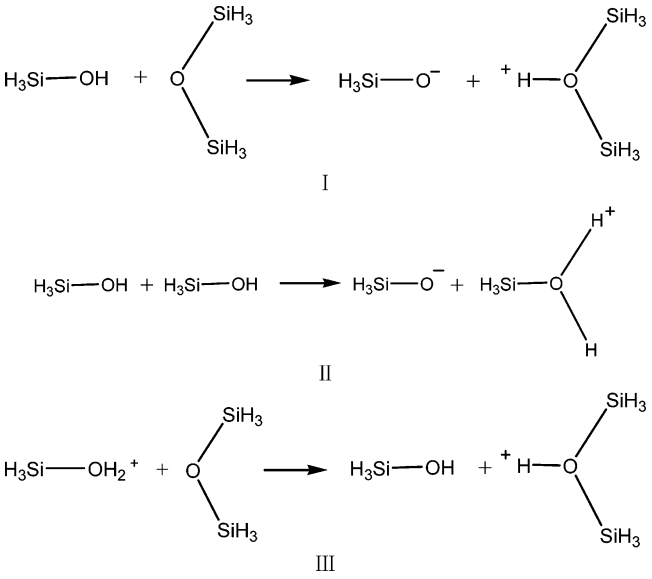

Figure 3. Proton-transfer reactions.

Table 7. Comparison of W1w Proton Affinities of Literatures Values (kcal/mol)

	present W1w	calculated G1 and G2[125]	Koput[124]
		Zero-Point Exclusive	
SiH_3O^-	363.7	363.3[a]	364.1 ± 1.1
SiH_3OH	184.2	184.3[a]	N/A
$(SiH_3)_2O$	186.3	185.9[a]	N/A
		ΔH_0	
SiH_3O^-	355.7	356.2[b]	356.2 ± 2
SiH_3OH	176.8	177.5[b]	N/A
$(SiH_3)_2O$	179.0	179.0[c]	N/A

[a] N/A denotes not available [b] G2 theory (ref 125) [c] G1 theory using MP2 for the 6-311+G(d,p) and 6-311G(d,p) basis set extensions (ref 125).

Table 8. Benchmark Values of Proton Affinities and Proton-Transfer Reaction Energies (Zero-Point Exclusive) at the W1w//B97-1/aug-cc-pV(T+d)Z Level

reaction	ΔE (in kcal/mol)
Proton Affinities	
$(H_3Si)_2OH^+ \rightarrow H^+ + (H_3Si)_2O$	186.3
$H_3SiOH_2^+ \rightarrow H^+ + H_3SiOH$	184.2
$H_3SiOH \rightarrow H^+ + H_3SiO^-$	363.7
Proton-Transfer Reaction Energies	
reaction I[a]	177.4
reaction II[a]	179.5
reaction III[a]	−2.1

[a] Reactions I, II, and III are illustrated in Figure 3.

The benchmark values for the protonation/deprotonation energies and the three proton-transfer reaction energies are give in Table 8. The MUEs of these proton affinities and proton-transfer reaction energies for high-level and multicoefficient methods are given in Table 9. All the errors in the tables are relative to the benchmark W1w results calculated using the geometries obtained at the B97-1/aug-cc-pV(T+d)Z level. The results obtained with DFT for the protonation/deprotonation energies and the overall proton-transfer reaction energies are given in Tables S4 and S5 (Supporting Information) and Table 10, respectively.

Table 9. Mean Unsigned Error of Three Proton Affinities and Three Proton Affinities and Three Proton-Transfer Reaction Energies by High-Level and Multicoefficient Methods (in kcal/mol)

	proton affinities	proton affinities and proton-transfer reaction energies
CCSD/MG3S	1.11	1.10
BMCCCSD//CCSD/MG3S	0.49	0.78
BMCCCSD//B97-1/aug-cc-pV(T+d)Z	0.49	0.57
MCG3/3 //CCSD/MG3S	1.12	0.86
MCG3/3//B97-1/aug-cc-pV(T+d)Z	1.07	0.83
W1w// CCSD/MG3S	0.05	0.05
W1w//B97-1/aug-cc-pV(T+d)Z	0	0

For proton affinities, the MIDIX+ basis set has the largest average MUE, in particular, 6.84 kcal/mol (Table S5, Supporting Information), and the MG3S basis set has the smallest average MUE, namely, 1.07 kcal/mol. The only functionals for which MG3S does not have the smallest error are the MPWLYP1M and M05-2X functionals. The functionals with a percentage of Hartree−Fock exchange less than or equal to 5% have MUEs systematically larger than those with 10% or more Hartree−Fock exchange. M05-2X with 56% HF exchange has the smallest average MUE values, in particular, 3.35 kcal/mol for polarized double-ζ basis sets and 0.23 kcal/mol using polarized triple-ζ basis sets. The same trends are observed in the MUEs of the three energies of the proton-transfer reactions in Figure 3. Tables S4 and S5 in the Supporting Information are full tables of the MUEs for the three proton affinities and the three energies of reaction, respectively, while Table 10 gives MUEs averaged over all six of these quantities. Table 10 shows that, for three proton affinities and three energies of reaction, MG3S has the smallest error in most DFT calculations, the exception being for the M05-2X functional. It is found that all of the average MUEs for polarized double-ζ basis sets are larger than 3 kcal/mol. The corresponding values for polarized triple-ζ basis sets are all 1.41 kcal/mol or less.

Among the polarized double-ζ basis sets, aug-pc1 is the largest and performs the best in many cases. MIDI! is the smallest basis, but it performs better than some bigger basis sets (6-31+B** and 6-31+G**). Among the polarized triple-ζ basis sets, MG3S is the best one for energies. MPW1B95 and M05-2X are the best functionals for energies with polarized double-ζ basis sets.

3.4. Composite Evaluation. In order to draw overall conclusions about the relative merits of the theoretical methods, we define a composite mean normalized percentage unsigned error as

$$\text{CMN\%UE} = [\text{MN\%UE(angles)} + \text{MN\%UE(distances)} + \text{MN\%UE(dipole moments)} + \text{MN\%UE(proton activity)}]/4 \quad (1)$$

Table 10. Mean Unsigned Error of Three Proton Affinities and Three Proton-Transfer Reaction Energies (in kcal/mol)

	X[a]	MIDI!	MIDIX+	6-31+B**	6-31+G**	aug-pc1	av (PDZ)[b]	MG3S	aug-pc2	aug-cc-pV(T+d)Z	av (PTZ)[b]
HCTH	0	3.56	4.74	5.24	5.01	3.96	4.50	2.04	2.50	2.48	2.34
M06-L	0	4.16	4.43	3.35	3.40	2.95	3.66	1.18	1.86	2.08	1.71
mPWPW	0	2.91	6.29	4.43	4.04	3.44	4.22	1.69	2.16	2.15	2.00
PBE	0	2.79	7.14	4.39	4.18	3.85	4.47	2.14	2.37	2.44	2.32
VSXC	0	3.54	5.58	3.86	3.73	3.00	3.94	1.72	1.93	1.98	1.88
MPWLYP1M	5	3.31	7.29	4.19	3.74	3.93	4.49	2.26	2.30	2.41	2.32
TPSSh	10	4.08	4.72	3.28	2.93	2.22	3.44	0.60	0.95	1.01	0.85
B3LYP	20	4.33	5.49	3.08	2.72	2.33	3.59	0.41	0.82	0.79	0.67
B97-1	21	4.21	4.77	3.82	3.62	2.44	3.77	0.88	1.38	1.26	1.17
B1LYP	25	4.59	5.30	3.01	2.75	2.14	3.56	0.22	0.60	0.56	0.46
M05	28	4.10	4.53	4.58	3.98	2.30	3.90	0.53	1.59	1.03	1.05
MPW1B95	31	4.47	5.04	2.78	2.48	1.61	3.28	0.31	0.55	0.36	0.41
PW6B95	46	4.48	4.96	3.10	2.76	1.85	3.43	0.34	0.77	0.58	0.56
M05-2X	56	4.95	4.79	2.34	2.38	1.60	3.21	0.46	0.13	0.25	0.28
MP2	100	4.08	6.61	3.68	3.50	2.82	4.14	1.58	0.89	1.47	1.31
av		3.97	5.44	3.68	3.41	2.70	3.84	1.09	1.39	1.39	1.29

[a] *X* denotes the percentage of Hartree−Fock exchange in the functional. [b] PDZ denotes polarized double-ζ; PTZ denotes polarized triple-ζ.

Table 11. Composite Mean Normalized Percentage Unsigned Error of 12 Geometrical Data, Dipole Moments, and Proton Activity Data on Basis of Calculations on Six Silicon-Containing Molecules

	X[a]	MIDI!	MIDIX+	6-31 B**	6-31+G**	aug-pc1	av (PDZ)[b]	MG3S	aug-pc2	aug-cc-pV(T+d)Z	av (PTZ)[b]
HCTH	0	6.00	10.20	9.52	7.39	6.73	7.97	1.53	2.28	2.02	1.94
M06-L	0	8.41	8.65	8.04	9.81	6.07	8.20	1.03	1.64	1.77	1.48
mPWPW	0	6.81	11.30	9.92	10.13	7.31	9.10	2.09	3.17	2.92	2.72
PBE	0	7.22	12.36	10.82	8.75	7.70	9.37	2.71	3.59	3.37	3.22
VSXC	0	6.90	11.05	10.40	9.94	7.01	9.06	3.61	3.76	3.54	3.63
MPWLYP1M	5	5.50	10.08	8.20	10.12	6.04	7.99	1.25	1.98	1.70	1.64
TPSSh	10	5.68	11.32	7.19	9.89	5.92	8.00	1.00	1.30	1.19	1.16
B3LYP	20	5.36	11.46	10.02	9.93	4.87	8.33	1.75	1.31	1.91	1.66
B97-1	21	6.46	10.25	9.19	10.03	6.20	8.42	0.78	1.79	1.45	1.34
B1LYP	25	5.09	11.47	10.03	9.97	4.59	8.23	2.12	1.67	2.21	2.00
M05	28	6.04	10.28	9.74	10.18	5.91	8.43	1.60	1.58	2.39	1.86
MPW1B95	31	5.89	11.26	8.49	9.72	5.15	8.10	1.54	1.15	1.70	1.47
PW6B95	46	5.63	11.23	6.17	9.70	5.13	7.57	1.63	1.24	1.77	1.55
M05-2X	56	6.10	11.80	8.96	10.09	5.29	8.45	0.79	1.24	0.98	1.00
MP2	100	9.02	13.32	12.76	12.19	10.29	11.52	3.36	3.68	3.76	3.60
av		6.41	11.07	9.30	9.86	6.28	8.58	1.79	2.09	2.18	2.02

[a] *X* denotes the percentage of Hartree−Fock exchange in the functional. [b] PDZ denotes polarized double-ζ; PTZ denotes polarized triple-ζ.

where the mean normalized percentage unsigned error of quantity Q is

$$\mathrm{MN\%UE}(Q) = \frac{\mathrm{MUE}(Q)}{\mathrm{MV}(Q)} \times 100\% \qquad (2)$$

and MV(Q) is the mean value of Q. For geometries, it can be calculated from Tables 4 and 5 that MV(angles) is 134.9°, and MV(distances) is 1.6395 Å. It can be calculated from Table 6 that MV(dipole moments) is 0.7835 D. The corresponding MUEs are in Tables 4−6. For proton activity, MV is the average of the absolute values of the six numbers in Table 8, which yields MV = 182.2 kcal/mol, and MUE is the value in Table 10.

Table 11 allows us to draw several important conclusions: (1) Polarized triple-ζ basis sets have errors about 4 times smaller than polarized double-ζ basis sets. Even the least accurate polarized triple-ζ basis set is about 3 times more accurate than the best double-ζ basis set. (2) MG3S is not only the smallest polarized triple-ζ basis set tested, it is also, on average, the most accurate. (3) MIDI!, although it was originally developed for Hartree−Fock calculations of geometries and charge distributions, and although it is the smallest polarized double-ζ basis set and has no diffuse functions, has a composite mean percentage error of only 6.35%, averaged over the functionals, which is better than three of the large polarized double-ζ basis sets and the same as the other, which has more than twice as many basis functions (see Table 2). (4) The most accurate density functional is M05-2X, which also has[71] excellent performance for a wide range of other quantities in main-group chemistry.

One reason for examining both local functionals (i.e., those with $X = 0$) and nonlocal functionals is that local functionals are more computationally efficient, especially when one uses density fitting,[128] which can only be used efficiently when $X = 0$. To illustrate this, we timed single-point energies on an oligo(dimethylsiloxane), namely, 3,5-tetramethyltetrasi-

loxane, with M05-2X (for which $X = 56$) and M06-L (for which $X = 0$), in both cases with the MG3S basis set, and in the latter case using density fitting. The ratio of computing times was a factor of 2.6. Furthermore, as the system size is increased and in the limit of large systems, the computing time for $X = 0$ scales as N^3, where N is the number of atoms, while that for $X \neq 0$ scales as N^4. Therefore, the reduction in cost when using local functionals can be quite significant for studying large silica systems.

In light of the favorable cost of local functionals, it is interesting to carry out a performance comparison focusing only on $X = 0$ functionals in Table 11. We see that the most accurate functionals at the polarized triple-ζ level are (in order) M06-L, HCTCH, mPWPW, and PBE. In fact, these four local functionals are all more accurate than MP2 (a WFT method), which scales as N^5.

4. Conclusions

A total of 14 DFT methods in combination with eight basis sets were assessed on a variety of properties, such as the structures, dipole moments, and proton affinities of disiloxane and silanol. For disiloxane conformers, the results obtained with the M05-2X functional in combination with polarized triple-ζ basis sets are in best agreement with the experimental and best estimate computational results. For silanol, the use of the MG3S basis set with DFT allows us to obtain values for several difficult properties that agree well with experimental results or high-level WFT. In particular, the M05-2X and M06-L calculations agree with the best estimates within, respectively, 1° and 4° for two bond angles, 0.002 and 0.003 Å for two bond distances, 0.01 and 0.02 D for two dipole moments, and 0.5 and 1.2 kcal/mol for six proton affinities and proton-transfer reaction energies.

On average, the most accurate density functional for both geometries and energetics is M05-2X, and M06-L is the most accurate local density functional. MIDI! is the smallest polarized double-ζ basis set tested but gives results in closer agreement, on average, with augmented polarized triple-ζ basis sets than do the more popular polarized double-ζ basis sets, and its performance is as good, on average, as the much larger aug-pc1 basis set. MG3S is not only the smallest polarized triple-ζ basis set tested, it is also, on average, the one that gives results closest to our best estimations of the correct values.

Acknowledgment. The authors are grateful to Dr. Mark Iron and Dr. Yan Zhao for assistance. This work was supported in part by the National Science Foundation under Grant No. ITR04-28774.

Supporting Information Available: Eight tables with key geometric parameters and error summaries for proton affinities and energies of proton-transfer reactions. This information is available free of charge via the Internet at http://pubs.acs.org.

References

(1) Tsuneyuki, S.; Aoki, H.; Tsukada, M. *Phys. Rev. Lett.* **1990**, *64*, 776.

(2) Warren, M. C.; Ackland, G. J.; Karki, B. B.; Clark, S. J. *Mineral. Mag.* **1998**, *62*, 558.

(3) Dubrovinsky, L.; Saxena, S. K.; Ahuja, R.; Johansson, B. *Geophys. Res. Lett.* **1998**, *25*, 4253.

(4) Tjabane, M.; Lowther, J. E. *Physica B* **1999**, *270*, 164.

(5) Kihara, K. *Phys. Chem. Miner.* **2001**, *28*, 356.

(6) Gibbs, G. V.; Cox, D. F.; Ross, N. L. *Phys. Chem. Miner.* **2004**, *31*, 232.

(7) Tsuchiya, T.; Caracas, R.; Tsuchiya, J. *Geophys. Res. Lett.* **2004**, *31*, L11610.

(8) Li, L.; Weidner, D. J.; Brodholt, J.; Alfè, D.; Price, G. D.; Caracas, R.; Wentzcovitch, R. *Phys. Earth Planet. Inter.* **2006**, *155*, 249.

(9) Wentzcovitch, R. M.; Tsuchiya, T.; Tsuchiya, J. *Proc. Natl. Acad. Sci. U.S.A.* **2006**, *103*, 543.

(10) Umemoto, K.; Wentzcovitch, R. M.; Allen, P. B. *Science* **2006**, *311*, 983.

(11) Ma, Y.; Garofalini, S. H. *Phys. Rev. B: Condens. Matter Mater. Phys.* **2006**, *73*, 174109.

(12) Sastre, G.; Corma, A. *J. Phys. Chem. B* **2006**, *110*, 17949.

(13) Susman, S.; Volin, K. J.; Price, L. D.; Grimsditch, M.; Rino, J. P; Kalia, R. K.; Vashishta, P.; Gwanmesia, G.; Wang, Y.; Liebermann, R. C. *Phys. Rev. B: Condens. Matter Mater. Phys.* **1991**, *43*, 1194.

(14) Tsuneyuki, S.; Matsui, Y. *Phys. Rev. Lett.* **1995**, *74*, 3197.

(15) Sarnthein, J.; Pasquarello, A.; Car, R. *Phys. Rev. Lett.* **1995**, *74*, 4682.

(16) Sarnthein, J.; Pasquarello, A.; Car, R. *Phys. Rev. B: Condens. Matter Mater. Phys.* **1995**, *52*, 12690.

(17) Pasquarello, A.; Car, R. *Phys. Rev. Lett.* **1997**, *79*, 1766.

(18) Benoit, M.; Ispas, S.; Jund, P.; Jullien, R. *Eur. Phys. J. B* **2000**, *13*, 631.

(19) Valle, R. G. D.; Venuti, E. *Phys. Rev. B: Condens. Matter Mater. Phys.* **1996**, *54*, 3809.

(20) Boureau, G.; Carniato, S.; Tetot, R.; Harding, J. H. *Mol. Simul.* **1997**, *20*, 27.

(21) Huang, L.; Duffrene, L.; Kieffer, J. *J. Non-Cryst. Solids* **2004**, *349*, 1.

(22) Hoang, V. V. *Diffus. Defect Data, Pt. A* **2005**, *242−244.*, 77.

(23) Zhao, D.; Feng, J. L.; Huo, Q.; Melosh, N.; Fredrickson, G. H.; Chmelka, B. F. *Science* **1998**, *279*, 548.

(24) Ying, J. Y.; Mehnert, C. P.; Wong, M. S. *Angew. Chem., Int. Ed.* **1999**, *38*, 56.

(25) Hatton, B.; Landskron, K.; Whitnall, W.; Perovic, D.; Ozin, G. A. *Acc. Chem. Res.* **2005**, *38*, 305.

(26) Earley, C. W. *J. Comput. Chem.* **1993**, *14*, 216.

(27) Nicholas, J. B.; Feyereisen, M. *J. Chem. Phys.* **1995**, *103*, 8032.

(28) Tielens, F.; Proft, F. D.; Geerlings, P. *THEOCHEM* **2001**, *542*, 227.

(29) Almenningen, A.; Bastiansen, O.; Ewing, V.; Hedberg, K.; Tretteberg, M. *Acta Chem. Scand.* **1963**, *17*, 2455.

(30) Nicholas, J. B.; Winans, R. E.; Harrison, R. J.; Iton, L. E.; Curtiss, L. A.; Hopfinger, A. J. *J. Phys. Chem.* **1992**, *96*, 7958.

(31) Stave, M. S.; Nicholas, J. B. *J. Phys. Chem.* **1993**, *97*, 9630.

(32) Pöhlmann, M.; Benoit, M.; Kob, W. *Phys. Rev. B: Condens. Matter Mater. Phys.* **2004**, *70*, 184209.

(33) Saengsawang, O.; Remsungnen, T.; Fritzsche, S.; Haberlandt, R.; Hannongbua, S. *J. Phys. Chem. B* **2005**, *109*, 5684.

(34) Chatterjee, A.; Iwasaki, T.; Ebina, T.; Tsuruya, H.; Kanougi, T.; Oumi, Y.; Kubo, M.; Miyamoto, A. *Appl. Surf. Sci.* **1998**, *130*−*132*, 555.

(35) McMillan, P. F. *Rev. Mineral.* **1994**, *30*, 131.

(36) Schiano, P.; Clocchiatti, R.; Shimizu, N.; Maury, R. C.; Jochum, K. P.; Hofmann, A. W. *Nature* **1995**, *377*, 595.

(37) Kohn, S. C. *Miner. Mag.* **2000**, *64*, 389.

(38) Bromile, G.; Hilaret, N.; McCammon, C. *Geophys. Res. Lett.* **2004**, *31*, L04610.

(39) Helms, C. R.; Poindexter, E. H. *Rep. Prog. Phys.* **1994**, *57*, 791.

(40) Friebele, E. J.; Griscom, D. L. *Mater. Res. Soc. Symp. Proc.* **1996**, *61*, 319.

(41) Gibbs, G. V.; Hill, F. C.; Boisen, M. B.; Downs, R. T. Molecules as a Basis for Modeling the Force Field of Silica. In *Structure and Imperfections in Amorphous and Crystalline Silicon Dioxide*; Devine, R. A. B., Duraud, J. P., Dooryhee, E., Eds.; John Wiley and Sons Ltd.: London, 2000; p 153.

(42) Bar, M. R.; Sauer, J. *Chem. Phys. Lett.* **1994**, *226*, 405.

(43) Banavar, J. R.; Phillips, J. C. *Phys. Rev. B: Condens. Matter Mater. Phys.* **1983**, *28*, 4716.

(44) Krishnamurty, S.; Pal, S.; Vetrivel, R.; Chandra, A. K.; Goursot, A.; Fajula, F. *J. Mol. Catal. A: Chem.* **1998**, *129*, 287.

(45) Ribeiro-Claro, P. J. A.; Amado, A. M. *THEOCHEM* **2000**, *528*, 19.

(46) Cheng, H.-P.; Barnett, R. N.; Landman, U. *J. Chem. Phys.* **2002**, *116*, 9300.

(47) Murashov, V. *J. Mol. Struct.* **2003**, *650*, 141.

(48) Simperler, A.; Bell, R. G.; Foster, M. D.; Gray, A. E.; Lewis, D. W.; Anderson, M. W. *J. Phys. Chem. B* **2004**, *108*, 7152.

(49) Abraham, R. J.; Grant, G. H. *J. Comput. Chem.* **1988**, *9*, 709.

(50) Feuston, B. P.; Garofalini, S. H. *J. Chem. Phys.* **1988**, *89*, 5818.

(51) Beest, B. W. H. v.; Kramer, G. J.; Santen, R. A. v. *Phys. Rev. Lett.* **1990**, *64*, 1955.

(52) Kramer, G. J.; Farragher, N. P.; Beest, B. W. H. v.; Santen, R. A. v. *Phys. Rev. B: Condens. Matter Mater. Phys.* **1991**, *43*, 5068.

(53) Becke, A. D. *J. Chem. Phys.* **1996**, *104*, 1040.

(54) Sun, H.; Rigby, D. *Spectrochim. Acta, Part A* **1997**, *53*, 1301.

(55) Smith, J. S.; Borodin, O.; Smith, D. G. *J. Phys. Chem. B* **2004**, *108*, 20340.

(56) Zhao, Y.; Truhlar, D. G. *J. Phys. Chem. A* **2004**, *108*, 6908.

(57) Nicholas, J. B.; Winans, R. E.; Harrison, R. J.; Iton, L. E.; Curtiss, L. A.; Hopfinger, A. J. *J. Phys. Chem.* **1992**, *96*, 10247.

(58) Nicholas, J. B.; Hess, A. C. *J. Am. Chem. Soc.* **1994**, *116*, 5428.

(59) Litton, D. A.; Garofalini, S. H. *J. Appl. Phys.* **2001**, *89*, 6013.

(60) Smith, J. S.; Bedrov, D.; Smith, G. D. *Macromolecules* **2005**, *38*, 8101.

(61) Demuth, T.; Hafner, J.; Benco, L.; Toulhoat, H. *J. Phys. Chem. B* **2000**, *104*, 4593.

(62) Zwijnenburg, M. A.; Bromley, S. T.; Alsenoy, C. v.; Maschmeyer, T. *J. Phys. Chem. A* **2002**, *106*, 12376.

(63) Tuma, C.; Sauer, J. *Chem. Phys. Lett.* **2004**, *387*, 388.

(64) Ernst, C. A.; Allred, A. L.; Ratner, M. A.; Newton, M. D.; Gibbs, G. V.; Moskowitz, J. W.; Topiol, S. *Chem. Phys. Lett.* **1981**, *81*, 424.

(65) Fernandez-Ramos, A.; Miller, J. A.; Klippenstein, S. J.; Truhlar, D. G. *Chem. Rev.* **2006**, *106*, 4518.

(66) Martin, J. M. L.; El-Yazal, J.; François, J.-P. *Mol. Phys.* **1995**, *86*, 1437.

(67) Jensen, F. *J. Chem. Phys.* **2001**, *115*, 9113.

(68) Lynch, B. J.; Zhao, Y.; Truhlar, D. G. *J. Phys. Chem. A* **2003**, *107*, 1384.

(69) Jensen, F.; Helgaker, T. *J. Chem. Phys.* **2004**, *121*, 3463.

(70) Curtiss, L. A.; Redfern, P. C.; Raghavachari, K. *J. Chem. Phys.* **2005**, *123*, 124107.

(71) Schultz, N.; Zhao, Y.; Truhlar, D. G. *J. Phys. Chem. A* **2005**, *109*, 11127. Zhao, Y.; Schultz, N. E.; Truhlar, D. G. *J. Chem. Theory Comput.* **2006**, *2*, 364. Furche, F.; Perdew, J. P. J. *Chem. Phys.* **2006**, *124*, 44103. Harvey, J. N. *Annu. Rep. Prog. Chem., Sect. C: Phys. Chem.* **2006**, *102*, 203.

(72) Nicholas, J. B. *Top. Catal.* **1997**, *4*, 157.

(73) Sauer, J.; Ahlrichs, R. *J. Chem. Phys.* **1990**, *93*, 2575.

(74) Becke, A. D. *Phys. Rev. A: At., Mol., Opt. Phys.* **1988**, *38*, 3098.

(75) Lee, C.; Yang, W.; Parr, R. G. *Phys. Rev. B: Condens. Matter Mater. Phys.* **1988**, *37*, 785.

(76) Adamo, C.; Barone, V. *Chem. Phys. Lett.* **1997**, *274*, 242.

(77) Stephens, P.; Devlin, F.; Chabalowski, C.; Frisch, M. *J. Phys. Chem.* **1994**, *98*, 11623.

(78) Hamprecht, F. A.; Cohen, A. J.; Tozer, D. J.; Handy, N. C. *J. Chem. Phys.* **1998**, *109*, 6264.

(79) Boese, A. D.; Doltsinis, N. L.; Handy, N. C.; Sprik, M. *J. Chem. Phys.* **2000**, *112*, 1670.

(80) Boese, A. D.; Handy, N. C. *J. Chem. Phys.* **2001**, *114*, 5497.

(81) Zhao, Y.; Schultz, N. E.; Truhlara, D. G. *J. Chem. Phys.* **2005**, *123*, 161103.

(82) Yan, Z.; Truhlar, D. G. *J. Chem. Phys.* **2006**, submitted.

(83) The mPW of the later versions of Gaussian 98 and of Gaussian 03 differs slightly from the early version of mPWPW91 of Gaussian 98 owing to an error in Gaussian's coding of the original mPW exchange functional. See http://www.gaussian.com/g_tech/g03_rel.htm#updatedman (accessed Dec 9, 2006) or http://comp.chem.umn.edu/info/mpw1k.htm (accessed Dec 9, 2006). We always use the correct version.

(84) Adamo, C.; Barone, V. *J. Chem. Phys.* **1998**, *108*, 664.

(85) Perdew, J. P.; Burke, K.; Ernzerhof, M. *Phys. Rev. Lett.* **1996**, *77*, 3865.

(86) Zhao, Y.; Truhlar, D. G. *J. Phys. Chem. A* **2005**, *109*, 5656.

(87) Staroverov, V. N.; Scuseria, G. E.; Tao, J.; Perdew, J. P. *J. Chem. Phys.* **2003**, *119*, 12129.

(88) Tao, J.; Perdew, J. P.; Staroverov, V. N.; Scuseria, G. E. *Phys. Rev. Lett.* **2003**, *91*, 146401.

(89) Voorhis, T. V.; Scuseria, G. E. *J. Chem. Phys.* **1998**, *109*, 400.

(90) Lynch, B. J.; Zhao, Y.; Truhlar, D. G. *J. Phys. Chem. A* **2005**, *109*, 1643.

(91) Hehre, W. J.; Radom, L.; Schleyer, P. v. R.; Pople, J. A. *Ab Initio Molecular Orbital Theory*; Wiley: New York, 1986.

(92) Easton, R. E.; Giesen, D. J.; Welch, A.; Cramer, C. J.; Truhlar, D. G. *Theor. Chim. Acta* **1996**, *93*, 281.

(93) Li, J.; Cramer, C. J.; Truhlar, D. G. *Theor. Chem. Acc.* **1998**, *99*, 192.

(94) Thompson, J. D.; Winget, P.; Truhlar, D. G. *Phys. Chem. Commun.* **2001**, *4*, 4116.

(95) Lynch, B. J.; Truhlar, D. G. *Theor. Chem. Acc.* **2004**, *111*, 335.

(96) Dunning, T. H. J.; Peterson, K. A.; Wilson, A. K. *J. Chem. Phys.* **2001**, *114*, 9244.

(97) Moller, C.; Plesset, M. S. *Phys. Rev.* **1934**, *46*, 618.

(98) Purvis, G. D.; Bartlett. R. J. *J. Chem. Phys.* **1982**, *76*, 1910.

(99) Lynch, B. J.; Truhlar, D. G. *J. Phys. Chem. A* **2003**, *107*, 3898.

(100) Martin, J. M. L.; Oliveira, G. d. *J. Chem. Phys.* **1999**, *111*, 1843.

(101) Oren, M.; Iron, M. A.; Burcat, A.; Martin, J. M. L. *J. Phys. Chem. A* **2004**, *108*, 7752.

(102) Martin, J. M. L. *THEOCHEM* **2006**, *771*, 19.

(103) Parthiban, S.; Martin, J. M. L. *J. Chem. Phys.* **2001**, *114*, 6014.

(104) Frisch, M. J.; Trucks, G. W.; Schlegel, H. B.; Scuseria, G. E.; Robb, M. A.; Cheeseman, J. R.; Montgomery, J. A., Jr.; Vreven, T.; Kudin, K. N.; Burant, J. C.; Millam, J. M.; Iyengar, S. S.; Tomasi, J.; Barone, V.; Mennucci, B.; Cossi, M.; Scalmani, G.; Rega, N.; Petersson, G. A.; Nakatsuji, H.; Hada, M.; Ehara, M.; Toyota, K.; Fukuda, R.; Hasegawa, J.; Ishida, M.; Nakajima, T.; Honda, Y.; Kitao, O.; Nakai, H.; Klene, M.; Li, X.; Knox, J. E.; Hratchian, H. P.; Cross, J. B.; Bakken, V.; Adamo, C.; Jaramillo, J.; Gomperts, R.; Stratmann, R. E.; Yazyev, O.; Austin, A. J.; Cammi, R.; Pomelli, C.; Ochterski, J. W.; Ayala, P. Y.; Morokuma, K.; Voth, G. A.; Salvador, P.; Dannenberg, J. J.; Zakrzewski, V. G.; Dapprich, S.; Daniels, A. D.; Strain, M. C.; Farkas, O.; Malick, D. K.; Rabuck, A. D.; Raghavachari, K.; Foresman, J. B.; Ortiz, J. V.; Cui, Q.; Baboul, A. G.; Clifford, S.; Cioslowski, J.; Stefanov, B. B.; Liu, G.; Liashenko, A.; Piskorz, P.; Komaromi, I.; Martin, R. L.; Fox, D. J.; Keith, T.; Al-Laham, M. A.; Peng, C. Y.; Nanayakkara, A.; Challacombe, M.; Gill, P. M. W.; Johnson, B.; Chen, W.; Wong, M. W.; Gonzalez, C.; Pople, J. A. *Gaussian 03*, revisions B.02, B.05, and C.02; Gaussian, Inc.: Wallingford, CT, 2004.

(105) Zhao, Y.; Truhlar, D. G. Minnesota-Gaussian Functional Module-version 2.0.1. http://comp.chem.umn.edu/mn-gfm/ (accessed Dec 9, 2006).

(106) Douglas, M.; Kroll, N. M. *Ann. Phys. (San Diego, CA, U.S.)* **1974**, *82*, 89. Hess, A. *Phys. Rev. A: At., Mol., Opt. Phys.* **1986**, *33*, 3742.

(107) Werner, H.-J. K. P. J.; Amos, R. D.; Bernhardsson, A.; Berning, A.; Celani, P. C. D. L.; Deegan, M. J. O.; Dobbyn, A. J.; Eckert, F.; Hampel, C.; Hetzer, G.; Korona, T. L. R.; Lloyd, A. W.; McNicholas, S. J.; Manby, F. R.; Meyer, W.; Mura, M. E. N. A.; Palmieri, P.; Pitzer, R.; Rauhut, G.; Schütz, M.; Schumann, U.; Stoll, H. S. A. J.; Tarroni, R.; Thorsteinsson, T. *MOLPRO*, version 2002.6; University of Birmingham: Birmingham, U. K., 2002.

(108) Nachtigall, P.; Jordan, K. D.; Smith, A.; Jonsson, H. *J. Chem. Phys.* **1996**, *104*, 148.

(109) Eichler, U.; Brandle, M.; Sauer, J. *J. Phys. Chem. B* **1997**, *101*, 10035.

(110) Tossell, J. A.; Sahaia, N. *Geochim. Cosmochim. Acta* **2000**, *64*, 4097.

(111) Walsh, T. R.; Wilson, M.; Sutton, A. P. *J. Chem. Phys.* **2000**, *113*, 9191.

(112) Yuan, S. P.; Wang. J. G.; Li, Y. W.; Peng, S. Y. *J. Mol. Catal. A: Chem.* **2002**, *178*, 267.

(113) Bussai, C.; Hannongbua, S.; Fritzsche, S.; Haberlandt, R. *Chem. Phys. Lett.* **2002**, *354*, 310.

(114) Tuma, C.; Sauer, J. *Chem. Phys. Lett.* **2004**, *387*, 388.

(115) Tossell, J. A. *Geochim. Cosmochim. Acta* **2005**, *69*, 283.

(116) Ginhoven, R. e. M. V.; Jonsson, H.; Park, B.; Corrales, L. R. *J. Phys. Chem. B* **2005**, *109*, 10936.

(117) Bakk, I.; Bóna, Á.; Nyulászi, L.; Szieberth, D. *THEOCHEM* **2006**, *770*, 111.

(118) Luke, B. T. *J. Phys. Chem.* **1993**, *97*, 7505.

(119) Durig, J. R.; Flanagan, M. J.; Kalasinsky, V. F. *J. Chem. Phys.* **1977**, *66*, 2775.

(120) Koput, J.; Wierzbicki, A. *J. Mol. Spectrosc.* **1983**, *99*, 116.

(121) Barrow, M. J.; Ebsworth, E. A. V.; Harding, M. M. *Acta. Crystallogr., Sect. B: Struct. Crystallogr. Cryst. Chem.* **1979**, *35*, 2093.

(122) Grigoras, S.; Lane, T. H. *J. Comput. Chem.* **1987**, *8*, 84.

(123) Coriani, S.; Gauss, J.; Hättig, C.; Helgaker, T.; Jørgensen, P. *J. Chem. Phys.* **2005**, *123*, 184107.

(124) Koput, J. *Chem. Phys.* **1990**, *148*, 299.

(125) Koput, J. *Chem. Phys. Lett.* **2001**, *333*, 504.

(126) Curtiss, L. A.; Brand, H.; Nicholas, J. B.; Iton, L. E. *Chem. Phys. Lett.* **1991**, *184*, 215.

(127) Damrauer, R.; Simon, R.; Krempp, M. *J. Am. Chem. Soc.* **1991**, *113*, 4431.

(128) Dunlap, B. I. *THEOCHEM* **2000**, *529*, 37.

(129) Varma, R.; MacDiarmid, A. G.; Miller, J. G. *Inorg. Chem.* **1964**, *3*, 1754.

CT6002884